IoT Structured Long-Term Wearable Social Sensing for Mental Wellbeing

Sihao Yang, Bin Gao, *Senior Member, IEEE*, Long Jiang, Jikun Jin, Zhao Gao, Xiaole Ma, and Wai Lok Woo

***Abstract*—Long-term wellbeing monitoring is an underlying theme for evaluating health status by collecting physiological signs through behavioral traits. In alignment with Internet of Things (IoT), nonintrusive and trustworthy wearable social sensing technology holds a potential way for researchers to find and establish the interrelationships between unobtrusive social cues and physical mental health. This paper implements an IoT structured wearable social sensing platform with the integration of privacy audio feature, behavior monitoring, and environment sensing in a naturalistic environment. Particularly, four privacy protected audio-wellbeing features are embedded into the platform to automatically evaluate speech information without preserving raw audio data. Four weeks of long-term monitoring experimental studies have been conducted. A series of well-being questionnaires in conjunction with a group of students are engaged to objectively investigate the relationships between physical and mental health by utilizing the feature fusion strategy from speech, behavioral activities, and ambient factors.**

***Index Terms*—Feature fusion and classification, Internet of Thing (IoT), long-term monitoring, mental health, wearable device.**

I. Introduction

HUMAN or environmental social signals can be used to assess a person's activity level, improve work efficiency, and understand human networks. In [1], by collecting social signals from the first 5 min of the negotiation, it is possible to predict the results with a high accuracy. Costa *et al.* [2] demonstrated that it is possible to help individuals to regulate emotions with mobile interventions that leverage the way human naturally react to bodily signal. In the fast-paced modern life, people face work and learning pressure. Research on mental health evaluation has attracted a lot of attention [3]–[6]. It is difficult to objectively evaluate a person's psychological state by directly using common questionnaire-based methods. The question of how to use social signal to evaluate a person's psychological state has unabatedly attracted researchers from various fields.

The rapid development of wearable devices is attributed to advances in sensor technology. Freescale uses MEMS to support sensor technology and analog device offers the integrated sensor components, including accelerometers, gyroscopes, sensor, and elastic measuring units that can be applied to detect and identify human behavior. In addition, sensors, such as temperature, humidity, light, and blood pressure are widely used in wearable devices because of the low power consumption and small size [9]–[11]. Wearable sensing can be used in many fields, such as motion recognition, physiological status, and pressure monitoring. They can be used in care service for the elderly, behavioral therapy [13], stress, and mental health monitoring. For long-term chronic diseases, doctors can remotely understand the patient's rehabilitation and health status by using wearable devices and Internet of Things (IoT) technology. Behavioral therapy refers to the monitoring of the rehabilitation for bad hobbies such as alcoholism. In [18], the wearable sensors consist of a neoprene band that contains circuitry for measuring electrodermal activity, three-axis motion, temperature, and electrocardiogram. In [20], for the assessment of emotions, anxiety, mood, depression, and stress, a head-mounted type was proposed by using electroencephalogram, chest band heart rate variability, and skin conductance sensors. In [26], the eyeball is tracked by a wearable device and the mental state of the person is detected by analyzing the activity of the eyeball. In order to objectively evaluate the human mental health, integrated sensors of mobile phone is applied [28]–[36]. Several apps, such as touch screen pressure perception [28], emotional *Q*-sensor [32], biomonitoring devices [31], [34], [35], and automatic sensing [36] are implemented to monitor both physiological and psychological status. More attention has been paid in mental health evaluation, several researchers already started to use wearable devices into this topic. Olguin *et al.* [7] designed a wearable badge to collect the wearer's voice and nonverbal information for assessing people's daily behavior. In [37], wearable devices are used to empower organizations and researchers to measure formal and informal social interaction across teams, divisions, and locations.

IoT has been applied to several different areas. Zanella *et al.* [45] have conducted a comprehensive survey of the enabling technologies, protocols, and architecture for

Manuscript received September 3, 2018; revised November 16, 2018; accepted December 17, 2018. Date of publication December 27, 2018; date of current version May 8, 2019. *(Corresponding author: Bin Gao.)*

S. Yang, B. Gao, L. Jiang, and J. Jin are with the School of Automation Engineering, University of Electronic Science and Technology of China, Chengdu 611731, China (e-mail: bin_gao@uestc.edu.cn).

Z. Gao is with the Clinical Hospital of Chengdu Brain Science Institute, MOE Key Laboratory for Neuroinformation, University of Electronic Science and Technology of China, Chengdu 611731, China, and also with the School of Foreign Languages, University of Electronic Science and Technology of China, Chengdu 611731, China.

X. Ma is with the Clinical Hospital of Chengdu Brain Science Institute, MOE Key Laboratory for Neuroinformation, University of Electronic Science and Technology of China, Chengdu 611731, China.

W. L. Woo is with the School of Engineering, Newcastle University, Newcastle upon Tyne NE1 7RU, U.K.

Digital Object Identifier 10.1109/JIOT.2018.2889966

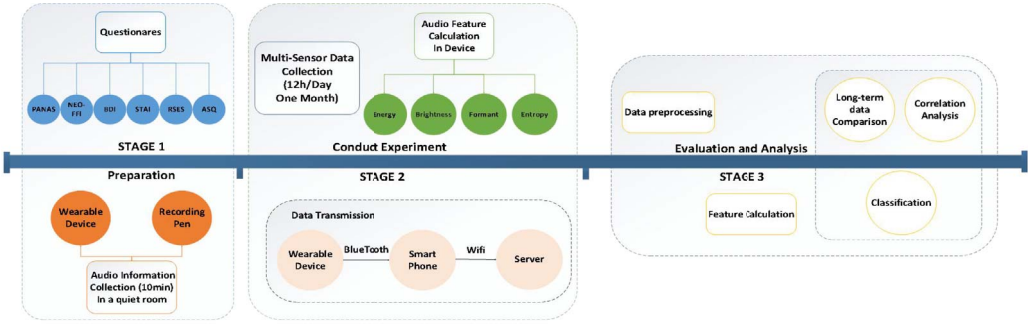

Fig. 1. Overall proposed architecture consisting of three stages.

an urban IoT. In [46], a wearable inertial sensor network and its associated activity recognition algorithm is proposed for recognizing human daily and sport activities. IoT has been applied to the medical and healthcare fields as ordinary citizens increasingly use these technologies to track sleep, food intake, activity, vital signs, and other physiological statuses. This activity is complemented by IoT systems that continuously collect and process environment-related data that has a bearing on human health. This synergy has created an opportunity for a new generation of healthcare solutions [5]. In [37], they present Rhythm, a platform that combines wearable electronic badges and online applications to capture team-level and network-level interaction patterns in organizations.

In previous studies, most research considered short-term data collection and analysis while the long-term social-mental health evaluation is rarely involved. In addition, there have been many studies on the privacy protection of wearable devices. Most of them are done from the data transmission protocol. Das *et al.* [47] presented a new lightweight authentication scheme suitable for wearable device deployment. In [48], the security issues of wearable devices were introduced and various lightweight authentication protocols for wearable devices were compared. In [49], they propose a new cloud-based user authentication scheme for secure authentication of medical data. Thus, it is necessary to conduct features extraction directly in the device to avoid the leakage of private information before transmission. Since IoT is a concept reflecting a connected set of anyone, anything, anytime, anyplace, any service, and any network, medical and healthcare represent one of the most attractive application areas for the IoT. Therefore, in this paper, we have developed a wearable social sensing watch that continuously extracts the original multiple sensing data while unobtrusively capturing social signals, including audio, behavioral, and environmental information. With an IoT capability, experiments have been conducted and data is collected for duration of 4 weeks.

This paper is divided into the following. Section II introduces the methodology. A brief introduction to the correlation analysis, the design and development of the experiments has been included. Evaluation and analysis are presented in Section III. In Section IV, we summarize the research work and indicate the future works.

II. Methodology and Experiment

Fig. 1 shows the overall architecture of the design platform. In Stage 1, we evaluate the psychological and mental status of all aspects of the participants in the form of questionnaires. In Stage 2, the participants wear wearable devices for 12 h a day within a month (4 weeks). In order to protect the privacy, four social-related features are extracted from the speech raw data, and finally only the speech features are saved. All the data collected by the wearable device is transmitted to the mobile phone via Bluetooth, and finally transmits the data to the background server via WiFi. In Stage 3, since experiment is completed, the collected multisensor data is first preprocessed and this is followed by features calculation, correlation analysis, and classification. In addition, we compare the data of the high and low scorer within day and month analysis. Through a series of experimental work, the relationship between social signals and mental state will be finally generated.

A. Wearable Device Platform

In order to collect the audio, behavioral, and environmental information without interfering the participant's living conditions, we design a multisensor integrated wearable device. Considering that there will be computational calculation involved in the device, a micro controller STM32F405 based on ARM-Cortex4 kernel has been selected which is an integrated DSP module. To facilitate real-time observation, we use OELD to display the sensor data. In addition, in order to achieve program debugging, data storage and transmission, JTAG debugging interface, SD card storage module, and Bluetooth module are designed. The whole system is powered by a lithium battery (3.7 V, 2200 mAh) and supplies power to each module through a voltage conditioning circuit. The overall hardware platform is shown in Figs. 2 and 3, respectively.

In Fig. 4, the framework of software is based on the open source operating system RT-thread real time operating system which uses a multithreaded mode to maximize CPU utilization. In the Audio-Thread, when collecting raw audio data, we use an analog to digital converter to sample and filter the digital signal of the audio code unit WM8978. In addition, the STM32F405 with the interintegrated circuit bus protocol of the WM8978 is used to control the amplification gain of the filtered audio signal.

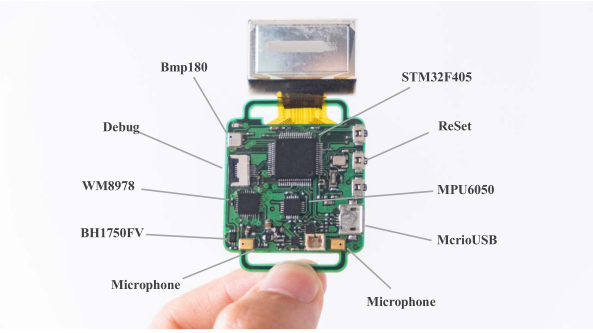

Fig. 2. Front view of the wearable device.

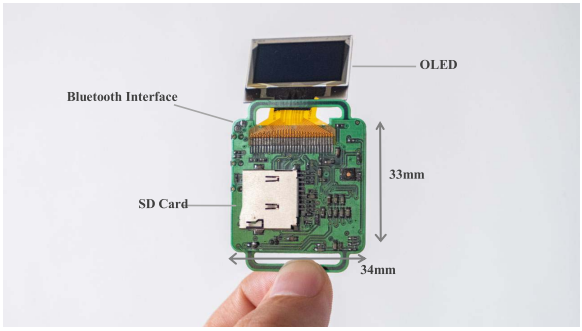

Fig. 3. Rear view of the wearable device.

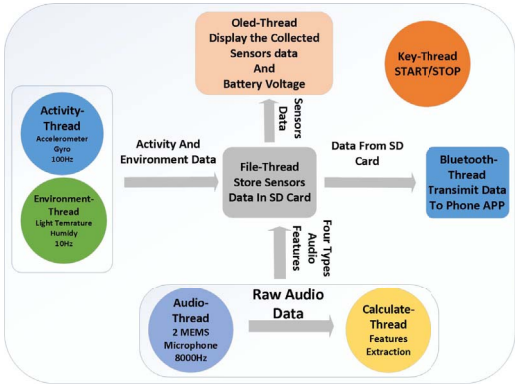

Fig. 4. Implementation framework of the software.

Since the raw audio data involves the privacy of the device user, we did not save the raw audio information. In Calculate-Thread, we extract the features of raw audio data in the wearable device. These audio features are related to social information, including energy, entropy, brightness [38], and formant [7]. In the File-Thread, the raw audio data will be deleted where only four type audio features are retained. In addition, in the Activity-Thread, the acceleration and gyro sensors are used to collect the motion information of the human body. In the Environment-Thread, the temperature, humidity, and light data in the environment are recorded. These sensor data will be temporarily stored in the SD card in File-Thread. In Bluetooth-Thread, data from the SD card can be transmitted to the phone via Bluetooth. The collected data and battery voltage values are displayed

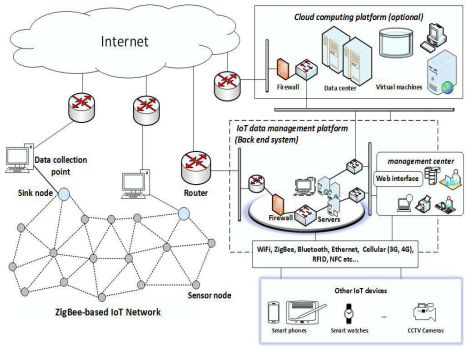

Fig. 5. Proposed IoT-enabled watch.

on the OLED via Oled-Thread, and the user can use the Key-Thread for human–computer interaction.

B. Data Collection and Transmission

In this paper, we use wireless sensing technology to connect with the wearable devices, mobile phones, and server databases, in Fig. 5. In this paper, we do not require real-time data transfer since analysis of the long-term monitor data is performed offline. In this way, the proposed platform not only provides us with the convenience of collecting data but the participants can also use the mobile app to view data collection and confirm that their privacy is protected.

C. Feature Calculation

1) Embedded Audio Social Features: The audio social feature extraction algorithm of DSP software library based on floating point computing unit of STM32F405 is summarized as follows.

1) The raw audio data is divided into N segments, each segment being approximately 30 ms. The short-term energy (EG) calculation formula for the ith frame audio signal is expressed as

$$\mathrm{EG}(i) = \sum_{n=0}^{L-1} h_i^2(n), \qquad 1 \le i \le fn. \tag{1}$$

The speech signal $h_i(n)$ is preprocessed by the Hamming window. L represents the frame length, which is the total number fn of frames after framing, representing the energy of the ith frame.

2) In order to obtain spectral entropy, the spectral probability density is first calculated before it can be used to calculate the short-term spectral entropy (EP) of the original audio signal frame. Here, we assume that the time-domain waveform of the noise-containing signal is $x(n)$, the ith frame speech signal obtained by Hamming window is $x_i(m)$, the energy spectrum of the kth spectral frequency component $f(k)$ is expressed as $Y_i(k)$ by applying fast Fourier transform (FFT) of $x_i(m)$. Can be obtained for each frequency component of the normalized spectrum probability density function

$$p_i(k) = \frac{Y_i(k)}{\sum_{l=0}^{N/2} Y_i(l)} \tag{2}$$

TABLE I
ERROR ANALYSIS

Audio Feature	Absolute Error
Energy	$0 \sim 4\times10^{-4}$
Entropy	$0 \sim 10\times10^{-5}$
Brightness	$0 \sim 10\times10^{-3}$
Formant	$0 \sim 55$

where $p_i(k)$ is the probability density of the kth frequency component $f(k)$ corresponding to the ith frame and N is the length of an FFT window. The short-term entropy spectrum of each analyzed audio frame is expressed as

$$\mathrm{EP}_i = -\sum_{k=0}^{N/2} p_i(k) \log p_i(k) \tag{3}$$

where EP_i is short-term spectral entropy calculated of the raw data of the ith frame.

3) In the audio data, the higher the correlation with the emotion is the brightness (B) feature, which is the centroid of the energy spectrum. The calculation formula of the brightness is as follows:

$$B = \frac{\int_0^{w_0} w|\mathrm{FP}(w)|^2 dw}{\int_0^{w_0} |\mathrm{FP}(w)|^2 dw} \tag{4}$$

where $\mathrm{FP}(w)$ is magnitude of a frequency point, w is the frequency corresponding to the spectral component. The following formula is expressed to calculate the discrete brightness (DB):

$$\mathrm{DB}_i = \frac{\sum_{k=0}^{N/2} w_k \cdot |y_k|^2}{\sum_{k=0}^{N/2} |y_k|^2} \tag{5}$$

where w_k is the frequency of the kth spectrum line, DB_i is ith frame brightness, y_k is the value of energy spectrum of the kth spectrum line.

4) To calculate the formant, we use cepstrum. The frame envelope is calculated using FFT and the inverse FFT. Among them, the maximum point of the calculated envelope is the formant parameter. A total of five formants are computed.

In order to provide specific comparison for the features in the wearable device with the features extracted on the PC, Table I demonstrates the error of the features calculated by the comparison.

As can be seen from Table I, the error range of energy and entropy is 0 to $4 \times 10 - 4$, the error range of brightness is 0 to $10 \times 10 - 3$, and the formant error range is 0 to 55 Hz. It can be found that the speech features extracted on the wearable device are correct.

2) Multimodal Sensing and Feature Extraction: Other multimodal sensing data are involved. We use motion and angular velocity (acceleration measurement range ± 4 g and gyroscope measurement range ± 2000 °/s) for motion analysis. Environmental information analysis will be carried out by using atmospheric pressure, ambient temperature, and photosensitivity; wrist skin temperature and humidity sensing for body data analysis. The relevant features are calculated in Table II.

TABLE II
MULTIMODAL SENSING AND FEATURE

Time Domain Feature Frequency Domain Feature

ID	Feature	Description of Feature
A	Mean	Average value of samples in a window
B	STD	Standard deviation of samples
C	Minimum	Minimum of samples in a window
D	Maximum	Maximum of samples in a window
E	Mode	The value with the largest frequency
F	Variance	Variance of samples in a window
G	Range	Maximum minus minimum
H	SMA	Signal magnitude area of 3-axis
I	DC	Direct component of a FFT window
J	Shape Features	Mean, STD, Skewness, Variance of shape about a FFT window
K	Amplitude Features	Mean, STD, Skewness, Variance, Kurtosis of amplitude about FFT

These are energy entropy, short-time energy, frequency-domain axis, standard deviation, mean, spacing, and correlation coefficient between rolling and peak. In this paper, we calculated a total of eight time domain features and ten frequency domain features.

To distinguish between the quiet state and the active state of the subject, we calculated the signal amplitude area (SMA), which is the sum of the areas surrounded by the three-axis (x, y, z) acceleration values. The calculation formula for SMA is

$$\mathrm{SMA} = \frac{1}{t}\left(\int_0^t |x(t)|dt + \int_0^t |y(t)|dt + \int_0^t |z(t)|dt\right) \tag{6}$$

where t is the time of samples in a window, $x(t)$, $y(t)$, and $z(t)$ are amplitude values of x-, y-, and z-axis, respectively.

Under the premise of ensuring accuracy and reducing computational complexity, we preprocessed the data of the original accelerometer. The synthetic acceleration is calculated as

$$a_i = \sqrt{\left(a_i^x\right)^2 + \left(a_i^y\right)^2 + \left(a_i^z\right)^2}, \quad i \in \{1, 2, \ldots n\} \tag{7}$$

where a_i is ith window synthetic acceleration, a_i^x, a_i^y, a_i^z represents triaxial (x-, y-, z-axis) accelerometer readings, respectively.

Activity feature is calculated from the sliding window. The block activity signal is divided into 50% overlap, a short period of time frame consisting of 285 sample points. The time interval between a set of activity features is 1 s, which makes it easy to get useful information under long-term monitoring. For example, in Fig. 6, the 2.6-h accelerometer raw data is collected to obtain the features of the time and frequency domains. Fig. 6 shows the Time Var and FFT Skew of these features.

D. Correlation Analysis

Before performing the correlation analysis, the social features (i.e., the score of questionnaire), audio features, and

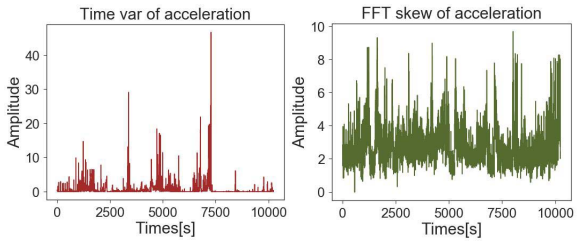

Fig. 6. Time Var (time domains) and FFT skew (frequency domain) of accelerometer data.

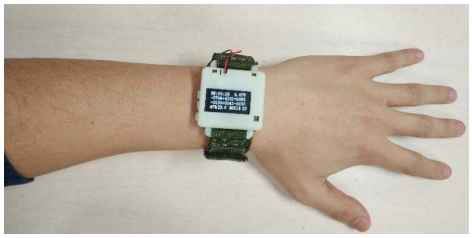

Fig. 7. Experimental participant wear wearable device.

activity features are summarized. The social features are obtained through questionnaire scores, a total of 22 features, and all autism spectrum (AQ) scores are involved between 11 and 34 points. For audio features, we calculate entropy, energy, five formants, the number of formants more than 0, brightness, nonzero formants average, formants' mean, formants' sum, and speaking time. A total of 36 activity features were calculated which included 18 accelerometer features and 18 gyroscope features. For these features, we calculated eight statistics, namely, sum, standard deviation, mean minimum, percentiles of 25%, 50%, 75%, and maximum. We use the previous threshold and calculate the two data of speech usage and ratio of daily activity time. Therefore, we obtain a total of 105 voice-related features and 289 behavior-related features. We use these features to perform four types of correlation analysis. In the general analysis, we analyze the correlation between 12 social features with audio features and activity features. The group correlation studies between AQ feature and audio features, AQ feature and activity features, and audio features and activity features are analyzed. The range of correlation value ranges from -1 to $+1$, where 1 represents a total positive linear correlation, 0 represents no correlation and -1 represents a total negative linear correlation. In addition, $0.8 \leq |r| \leq 1$ represents high correlation, $0.5 \leq |r| < 0.8$ represents moderate correlation, $0.3 \leq |r| < 0.5$ represents low correlation and $|r| \leq 0.3$ represents weak correlation.

E. Experiment

1) Support Assessment: In order to ensure the validity of the experimental data, when selecting the experimental participant before conducting the experiment, they need to fill out a questionnaire for evaluating their personality characteristics and emotional state. A total of six types of questionnaires are included. Using the scale (PANAS) [39], the participants can be assessed for their positive and negative attitudes and indirectly assessed their cognitive and emotional well-being, with a total of two scales. Using the neuroticism extraversion openness to experience five-factor inventory (NEO-FFI) [41], participant can be tested with person's personality characteristics, including neuroticism, extroversion, openness, agreeableness, and Conscientiousness. The beck depression inventory (BDI) is a multichoice self-reporting stock of 21 questions and it is the most widely used psychological test for measuring depression levels. The evaluation of anxiety is divided into state anxiety and trait anxiety. State anxiety refers to the anxiety generated by the tester in a special state, such as feeling threatened, and trait anxiety refers to the degree of anxiety of people in normal daily life and experience. The tester is required to complete a state-trait anxiety inventory (STAI) containing 40 self-reported questions. The Rosenberg self-esteem scale [42] is a self-esteem scale that is widely used in social science research to assess personal characteristics. A preliminary judgment of adult autism tendencies, AQ [44] has a good predictive effect, we can use this questionnaire to evaluate a normal intellectual adult with AQ.

2) Experiment Setup: Experimental participants will be tested before the start of the experiment. The purpose of the premental health related experiments is for testing the trust, medication, bad hobby, and living habit of the participants. This will guarantee that the selected participants are able to complete the whole experiments. In addition, the experimental studies are conducted by professional psychologists and all volunteers are preinterviewed for the selection procedure by these researchers to obtain an initial evaluation. All chosen volunteers would sign an experiment informed agreement before conducting the experiment. The detailed experimental procedure and equipment usage are briefed to them. Additionally, ethics approval information has been included in the experimental informed agreement.

At the beginning of the experiment, participant will come to a quiet room for a speech of more than about 10 min for experiment instruction process. We will use the wearable device and external recording equipment to record at the same time. Participant will then complete the PANAS, STAI, NEO-FFI, RSE, BDI, and AQ questionnaires to determine if they are suitable for this experiment, and based on the AQ scores of the subjects, we have chosen 16 participants participated in the experiment (average age 22, 8 undergraduate students, 8 graduate students; 15 males and 1 female), which were divided into AQ high group (AQ $>$ 25) and low group (AQ $<$ 25). The participant needs to wear the device correctly for 12 h a day and needs to complete an activity log table every day. A series of questionnaires filled out during the start of the experiment are repeated each week to record changes in their emotional state. The duration of this experiment is one month (4 weeks). If there is a special reason in the middle, the experiment cannot be performed, and the wearing time is postponed until the experimental days reach one month.

The main purpose of the experiment is to use long-term data collected by wearable devices to determine the relations between these sensor data and mental state. Fig. 7 shows an example of the test participant. The score of the AQ questionnaire provides us with an individual's level of autism symptoms [44].

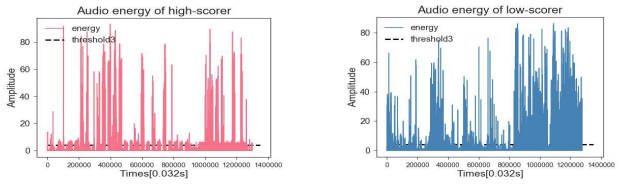

Fig. 8. Audio energy thresholds of high and low AQ scorer.

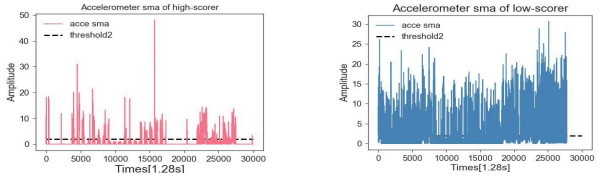

Fig. 9. Accelerometer SMA thresholds of high and low AQ scorer.

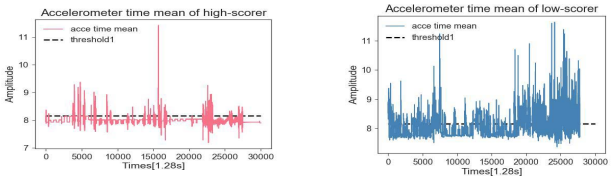

Fig. 10. Accelerometer time mean thresholds of high and low AQ scorer.

III. Evaluation and Analysis

A. Threshold Selection

We use the data collected by wearable devices to analyze the relationship between these data and social behavior as well as social interaction. In order to extract the useful time period data from the raw data, we calculate the activity time period of the equipment user by the SMA and the energy of the accelerometer (time average of the accelerometer). In addition, we can estimate the length of time of the audio by the energy of the short-term audio during one day of monitoring.

According to the real situation, by measuring in a quiet environment, our threshold selection for SMA is 8.16, the threshold of energy for accelerometer is 2, and the threshold for short-term audio energy is 4. By selecting the threshold, most of the noise in the data can be removed. Through these values, we can determine whether the device user is walking or communicating with others.

In Figs. 8–10, the AQ high scorer and low scorer are compared. It is apparent from the figure that the high scorer's day (10 h) activity and speech use time (activity time 51 min, speech use 28 min) is less than low scorer (activity behavior 223 min, speech use 52 min). When conducting long-term monitoring (4 weeks) experiments, the data were divided by these thresholds, and the correlation between mental health questionnaire scores and social characteristics was significantly improved.

B. Correlation Analysis

1) General Analysis: In the Table III, the correlation coefficients between the audio features and 12 different questionnaires are given where "numbers" represents the number of audio features whose absolute value is higher than 0.5 or

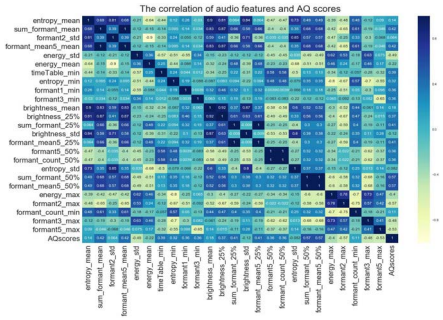

Fig. 11. Correlation coefficient heat map of audio features and AQ scores.

0.6. It is clear from the table that the formant is almost related to all social features (e.g., the absolute value of the correlation coefficient is higher than 0.5). It is found that each of the audio features (energy, entropy, brightness, and formant) is at least associated with at least one questionnaire score. Among the many questionnaire features, the number of audio features related to TAI and Conscientiousness is the highest (19). The most relevant audio feature to TAI is sum_formant_mean (0.75), and for Conscientiousness it is formant_mean_min (-0.90). In addition, there is a positive correlation between the AQ score and the TAI score, the correlation coefficient is 0.49, and there is a negative correlation between the AQ score and Conscientiousness, and the correlation coefficient is -0.78. Therefore, it can be seen that AQ high scorers may be more anxious and less responsible. In Table IV, the correlation coefficients between behavioral features and 12 different questionnaire scores are given. The correlation between the behavioral features listed and the score of the questionnaires is higher than 0.5. It can be found that the behavioral features are highly correlated with the questionnaires score, both in the frequency domain and in the time domain. Moreover, the number of behavioral features closely related to AQ scores is the highest (up to 20). In addition, most of these behaviors are negatively correlated with AQ scores where it can be seen that people with higher AQ have fewer activities and do not often move around.

2) Speech Analysis and AQ Scores: Fig. 11 is a correlation coefficient heat map of audio features and AQ scores. As can be seen from the figure, the absolute value of the correlation coefficient of the six audio features and AQ is about 0.5, they are formant2_max is -0.57, formant3_max is -0.48, formant5_max is -0.53, sum_formant_50% is 0.57, energy_std is -0.49, and formant_mean5_50% is 0.57. Formant2_max represents the maximum value of the second formant, forant3_max represents the maximum value of the third formant, formant5_max represents the maximum value of the fifth formant, sum_formant_50% represents the sum of the 5 formants, and energy_std represents the standard deviation of short-term energy, formant_mean5_50% represents the average of five formants. It can be found that we can distinguish between the high scorer and the low scorer of AQ by energy features and formant features.

3) Activity Analysis and AQ Scores: Fig. 12 is a correlation coefficient heat map of behavioral features and AQ score. It can be seen from the figure that both

TABLE III
CORRELATION RESULTS BETWEEN AUDIO FEATURES AND THE SCORES OF 12 DIFFERENT PSYCHOLOGICAL QUESTIONNAIRES

Questionnaires	Correlation Features （|Correlation| > 0.5 or |Correlation| > 0.6）		
	|Correlation|	Numbers	Audio Features (correlation value)
AQ	>0.5	3	sum_formant_50% (0.56), formant2_max (-0.57), formant5_max (-0.53)
Positive	>0.5	6	sum_formant_mean (-0.65), timeTable_75% (0.55), energy_max (0.56) formant2_max (0.56), formant3_max (0.53), formant5_max (0.50)
Negative	>0.5	6	formant4_mean (-0.63), brightness_min (-0.53), sum_formant_max (0.57) formant_count_25% (-0.75), entropy_std (0.68), formant3_75% (0.53)
SAI	>0.5	4	formant1_std (-0.51), brightness_75% (-0.50), formant4_25% (-0.57), formant_count_25% (-0.56)
TAI	>0.6	5	sum_formant_mean (0.75), brightness_75% (-0.62), formant2_min (0.55)
	>0.5	19	entropy_75% (0.52), timeTable_std (-0.59), formant1_max (-0.53)
Neuroticism	>0.5	3	formant mean min (0.61), sum formant 75% (0.51), formant2 75% (0.53)
Extraversion	>0.5	3	energy std (0.61), timeTable min (-0.78), sum formant 25% (-0.59)
Openness	>0.5	6	formant mean mean (-0.53), formant count 75% (0.69), formant1 max (0.52)
Agreeableness	>0.5	3	sum_formant_mean (-0.59), formant2_75% (-0.52), formant_mean_75% (-0.52)
Conscientiousness	>0.6	8	entropy_mean (-0.61), brightness_mean (-0.71), formant2_mean (-0.75)
	>0.5	19	formant mean5 mean (-0.82), timeTable std (0.64), formant mean min (-0.90)
SES	>0.5	9	formant1_75% (-0.57), formant2_75% (-0.60), formant3_75% (-0.50) formant4_75% (-0.54), energy_std (-0.58), formant_count_50% (0.58)
BDI	>0.5	3	timeTable_75% (-0.53), timeTable_min (0.51), sum_formant_50% (0.69)

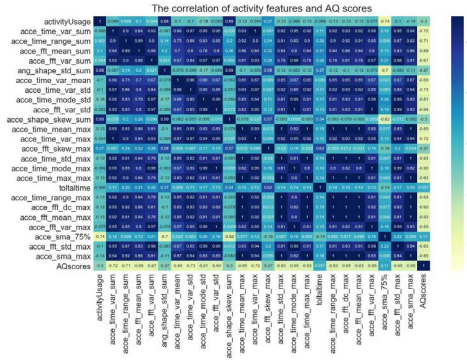

Fig. 12. Correlation coefficient heat map of activity features and AQ scores.

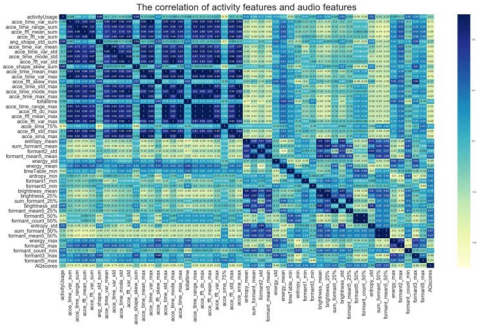

Fig. 13. Correlation coefficient heat map of activity features and audio features.

the frequency domain and the time domain features have a high correlation with AQ. The absolute values of the correlation coefficients of the four behavioral features of acce_time_var_sum, acce_time_range_sum, acce_time_var_std, acce_time_var_max, and AQ score exceed 0.7.

4) Activity Analysis and Audio Analysis: Fig. 13 shows a heat map of the correlation coefficients of behavioral features and audio features. As can be seen from the figure, the audio features have a high correlation with the behavioral features, and most of them are negatively correlated. The absolute values of the correlation coefficients of the audio feature entropy_mean and acce_time_range_sum, acce_fft_mean_sum, acce_time_mean_max, acce_time_std_ max, acce_time_max_max, toltal_time, acce_time_range_ max, acce_fft_dc_max, acce_fft_mean_max, and acce_sma_max are all higher than 0.5, where entropy_mean and toltal_time are −0.77. There are high correlation coefficient of audio feature sum_formant_mean with a total of 19 behavioral features. The correlation coefficient of a total of 19 behavioral features, such as audio feature formant_mean5_mean and acce_time_var_mean is greater than 0.5. There are 19 behavioral features, such as acce_time_var_mean, etc., the absolute values of their correlation coefficients with audio feature formant_mean5_mean are greater than 0.5. Brightness_mean and Brightness_25%, respectively, with 11 behavioral features, such as acce_time_range_max, total time, etc. A total of 11 feature correlation coefficients have an absolute value greater than 0.5. The absolute value of the correlation between audio feature entropy_std and 16 behavioral features is almost equal to 0.5. The sum_formant_50% and the formant_mean5_50% have a high correlation with up to 24 behavioral featrures, in particular, they are 0.71 with acce_time_range_sum and 0.74 with acce_fft_mean_sum. Through analysis, the seven audio features of entropy_mean, sum_formant_mean, formant_mean5_mean, brightness_mean, brightness_25%, entropy_std, sum_formant_50%, and formant_mean5_50% have a strong negative correlation with most behavioral features that are highly correlated with AQ.

C. Long Time Analysis

1) High AQ Group Versus Low AQ Group in Day: We calculated the kernel density estimate and plotted the density curves of social characteristics to compare the differences in social characteristics between AQ high scorers and low scorers. In Figs. 14–17, the 2nd audio formant, accelerometer FFT mean, accelerometer shape variance, and the accelerometer time variance are compared for one day of high scores and low scores. As can be seen from the figure, the images of the high scorers are relatively dense, while the low scorers are sparse. The value of acce_time_var in a day of 80% of AQ high scorers is between 0 and 40, while the value of acce_time_var of most AQ low scorers is close to zero. It can be seen that although the FFT mean of the accelerometers

TABLE IV
CORRELATION RESULTS BETWEEN ACTIVITY FEATURES AND THE SCORES OF 12 DIFFERENT PSYCHOLOGICAL QUESTIONNAIRES

Questionnaires	Correlation Features （|Correlation| > 0.5）	
	Numbers	Activity Features (correlation value)
AQ	20	acce_time_var_sum (-0.72), acce_fft_mean_sum (-0.69), acce_fft_dc_max (-0.65), acce_shape_var_max (-0.55)
Positive	11	acce_time_std_sum (0.68), acce_fft_mean_sum (0.61), acce_sma_sum (0.63), acce_shape_skew_max (0.51)
Negative	1	ang_time_mode_max (0.62)
SAI	4	acce_time_std_sum (-0.71), acce_time_range_sum (-0.61), acce_fft_mean_sum (-0.66), acce_fft_std_sum (-0.56)
TAI	18	acce_fft_var_mean (-0.65), acce_fft_var_sum (-0.78), timeTable_50% (-0.56), acce_sma_max (-0.59)
Neuroticism	4	acce_fft_var_mean (-0.65), acce_time_mode_std (-0.67), acce_time_var_sum (-0.50), acce_time_mode_max (-0.63)
Extraversion	3	acce_fft_skew_mean (-0.51), acce_fft_kurt_mean (-0.57), ang_time_min_50% (-0.54)
Openness	12	ang time var mean (0.54), ang time range std (0.61), acce fft dc 50% (-0.54), ang fft mean max (0.51)
Agreeableness	7	ang fft skew mean (0.51), ang fft kurt mean (0.57), acce time mean 25% (-0.56), acce fft dc 50% (-0.60)
Conscientiousness	14	acce_fft_std_std (0.67), ang_time_min_std (0.58), ang_time_range_min (0.51), timeTable_50% (0.56)
SES	16	acce_fft_var_mean (0.60), acce_sma_min (0.56), ang_fft_kurt_min (-0.51), ang_time_range_min (0.58)
BDI	4	acce_time_std_sum (-0.53), ang_time_mean_std (0.55), ang_shape_var_min (0.51), acce_fft_var_75% (0.50)

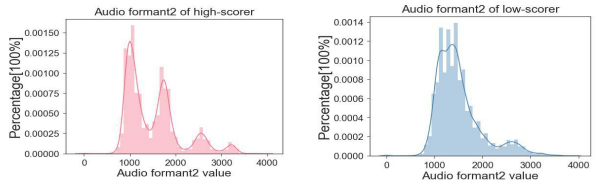

Fig. 14. Audio formant2 of high and low AQ scorer.

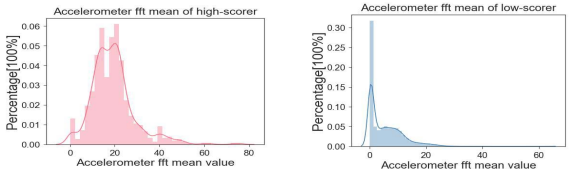

Fig. 15. Accelerometer FFT mean of high and low AQ scorer.

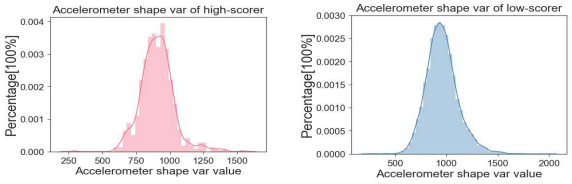

Fig. 16. Accelerometer shape variance of high and low AQ scorer.

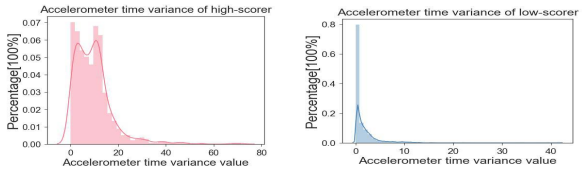

Fig. 17. Accelerometer time variance of high and low AQ scorer.

of the AQ group and the accelerometer have the same trend, the maximum values of the two are not the same. The maximum score of the high score is 1500, while the score of the low scorer is low. The maximum value is about 2000. There is a significant difference in the second-frequency formant of the two participants meantime.

2) AQ High-Scorers Versus AQ Low-Scorers During Month: See Fig. 18.

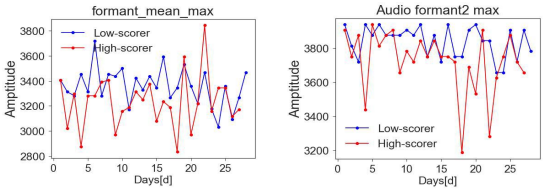

Fig. 18. Comparison of formant_mean_max and formant2_max in high and low scores during one month.

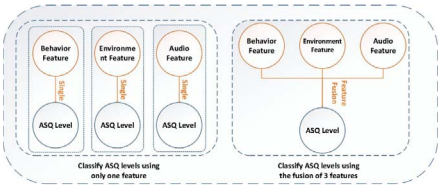

Fig. 19. AQ level is classified using only one feature and feature fusion.

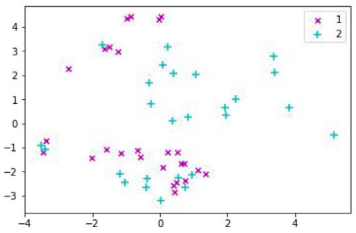

Fig. 20. Sample point of environmental feature distribution after PCA.

D. Classification

Through the calculation of features, 291 human behavioral features, 289 environmental features, and 107 audio features were obtained. As participants filled in the AQ questionnaire four times during the experiment, we judge their AQ level according to the scores in the questionnaire.

Among all, there exists a lot of redundant features. Therefore. In order to avoid unnecessary calculation, the 2-D PCA is used to reduce the dimensions of audio, behavior, and environmental features in Fig. 20.

First, we use only one of the features of audio, environment, or behavior to classify AQ levels. Participants fill out the AQ questionnaire every week, and we found that their AQ scores did not change much. In Fig. 21, the AQ scores of seven of the participants were shown, the final AQ score of the participants is obtained by averaging four times.

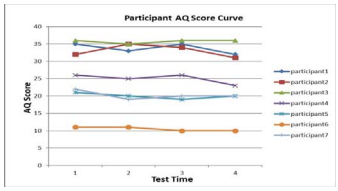

Fig. 21. AQ scores of seven participants.

TABLE V
DIVIDE AQ LEVEL (MAX = AQ_SCORE_MAX, MIN = AQ_SCORE_MIN)

AQ Level(Lable)	AQ questionnaire score(S)
1	Min≤S＜Min+gap
2	Min+gap≤S＜Max

gap=(AQ_Score_max-AQ_Score_min)/2).

TABLE VI
DIFFERENT FEATURE CLASSIFICATION RESULTS

Feature	Accuracy
Audio	0.87
Behavior	0.67
Environment	0.56

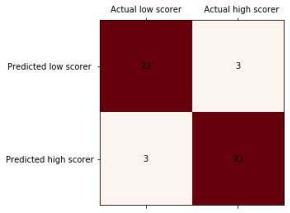

Fig. 22. Confusion matrix.

TABLE VII
COMBINE AUDIO, BEHAVIOR, AND ENVIRONMENT FEATURE USING LR

Feature	Accuracy
Fusion feature	0.90

The label of training data is marked according to the score of AQ questionnaire. In Table V, we divide AQ level into two classes.

We use logistic regression (LR) classifier to classify. In order to obtain as much effective information as possible from limited data, to test the performance of the trained model on new data and to avoid over-fitting, k-cross fold validation is used. The result shows in Table VI.

As can be seen from the results, the classification of each feature alone is not satisfactory. Although the data has been preprocessed before the calculation, since this experiment is a long-term monitoring, there will be a lot of noise in the data. And the experimenter not only wears the equipment in a specific occasion, they wear it all the time, which is also subject to great interference, and the degree of interference is not the same.

In Fig. 19, because the mental state is related to the social signals, such as audio, behavior, and environment, it is interesting to combine all three features for analysis and the classifier selects the LR classifier. The result are shown in Table VII and confusion matrix is shown in Fig. 22, this is a 2-D confusion matrix, the numbers in the matrix represent the number of samples.

By using fusion feature to classify, the accuracy has been improved. It can be seen from the classification results that people's mental and psychological conditions are related to audio, behavior, and the environment. So we can use such multisensing wearable devices to objectively assess a person's mental health.

E. Discussion

1) Why Choose College Students as Participants: In recent years, there has been a growing concern about mental health issues on college students. From the statistics calculation of our psychologist researchers, this number is growing fast. In addition, the procedure of collecting long-time data are cumbersome and complicated.

In future work, the experiment variables, such as different age groups and number of participants will be studied. In addition, we have recently started to cooperate with specialized psychotherapy hospitals and to recruit genuine patients for in-depth study. This will be the subject of future investigation which leverages the knowledge acquired from the current preliminary work.

2) Long-Term and Short-Term: Both short and long term studies have potential significant value for deep mining. The analysis of the short-term data has been previously studied in this paper [38]. In this paper, we consider that it is unsubstantial to judge that long-term study is better than that of short-term study as they reflects the two aspects, namely, short-term analysis reflects the temporal emotion behavior within a specialized situation while long-term study provides assessment on psychological changes and trends during a period where the similarities and differences between AQ high scorers and low scorers can be statistically distinguished. As discussed, a person may deliberately disguise his emotions with short-term behavior. On the other hand, this can temporal objectively reflects their emotion and mental state. The purpose of this paper is to determine whether a person's psychological state can be statistically monitored over a longer term trend in the overall data. Long-term data monitoring can avoid one's subjective emotional control during the period of time which increases the reliability of the results by averaging. In addition, the volunteers wear the equipment from morning until night, migrate over different places and environments in a completely natural daily situation in which the collected data is not limited in a specific situation. This provides increased reliability in analyzing peoples' social behave in an objective way. Thus, as organized by psychologist researchers, short-term data suffers from noise interference as well as limited situations which may lead to the immature judgment. This experimental mode of long-term natural wear resembles more closely to real life.

IV. CONCLUSION

In this paper, we have designed an IoT-based wearable device that integrates multiple sensors. Using this device, we monitored the experimenter for a long time. In order to collect

and visualize data, we have developed app based on android phones and server. In wearable devices, we have extracted the features from the original voice to protect users' privacy. Through the analysis of the long time detection data, the classification algorithm is applied to classify the user AQ level. Through the conducted research, it is shown that there are significant connections between physical information and participant's psychological state. Participant can use wearable devices to monitor their psychological conditions so that their behavior can be timely adjusted. In the future study, more experiments will be conducted in wide age group and real patients to improve reliability of the proposed method.

REFERENCES

[1] S. Abdullah, M. Czerwinski, G. Mark, and P. Johns, "Shining (blue) light on creative ability," in *Proc. ACM Int. Joint Conf. Pervasive Ubiquitous Comput.*, 2016, pp. 793–804.

[2] J. Costa, A. T. Adams, M. F. Jung, F. Guimbretiere, and T. Choudhury, "EmotionCheck: Leveraging bodily signals and false feedback to regulate our emotions," in *Proc. ACM Int. Joint Conf. Pervasive Ubiquitous Comput.*, 2016, pp. 758–769.

[3] S. M. R. Islam *et al.*, "The Internet of Things for health care: A comprehensive survey," *IEEE Access*, vol. 3, pp. 678–708, 2015, doi: 10.1109/Access.2015.2437951.

[4] S. Boll, J. Meyer, and N. E. O'Connor, "Health media: From multimedia signals to personal health insights," *IEEE Multimedia*, vol. 25, no. 1, pp. 51–60, Jan./Mar. 2018.

[5] A. Sheth, U. Jaimini, and H. Y. Yip, "How will the Internet of Things enable augmented personalized health?" *IEEE Intell. Syst.*, vol. 33, no. 1, pp. 89–97, Jan./Feb. 2018.

[6] G. Yang *et al.*, "IoT-based remote pain monitoring system: From device to cloud platform," *IEEE J. Biomed. Health Informat.*, vol. 22, no. 6, pp. 1711–1719, Nov. 2018, doi: 10.1109/JBHI.2017.2776351.

[7] D. O. Olguin *et al.*, "Sensible organizations: Technology and methodology for automatically measuring organizational behavior," *IEEE Trans. Syst., Man, Cybern. B, Cybern.*, vol. 39, no. 1, pp. 43–55, Feb. 2009.

[8] A. Nag, S. C. Mukhopadhyay, and J. Kosel, "Wearable flexible sensors: A review," *IEEE Sensors J.*, vol. 17, no. 13, pp. 3949–3960, Jul. 2017.

[9] S. Patel, H. Park, P. Bonato, L. Chan, and M. Rodgers, "A review of wearable sensors and systems with application in rehabilitation," *J. Neuroeng. Rehabil.*, vol. 9, no. 1, p. 21, 2012.

[10] X.-F. Teng, Y.-T. Zhang, C. C. Y. Poon, and P. Bonato, "Wearable medical systems for p-health," *IEEE Rev. Biomed. Eng.*, vol. 1, pp. 62–74, 2008.

[11] P. Bonato, "Wearable sensors and systems. From enabling technology to clinical applications," *IEEE Eng. Med. Biol. Mag.*, vol. 29, no. 3, pp. 25–36, May/Jun. 2010.

[12] J. C. Torrado, J. Gomez, and G. Montoro, "Emotional self-regulation of individuals with autism spectrum disorders: Smartwatches for monitoring and interaction," *Sensors*, vol. 17, no. 6, p. 1359, 2017.

[13] R. R. Fletcher, M. Z. Poh, and H. Eydgahi, "Wearable sensors: Opportunities and challenges for low-cost health care," in *Proc. IEEE Conf. Eng. Med. Biol. Soc.*, 2010, pp. 1763–1766.

[14] E. Bekele *et al.*, "Multimodal adaptive social interaction in virtual environment (MASI-VR) for children with autism spectrum disorders (ASD)," in *Proc. IEEE Vir. Real.*, 2016, pp. 121–130.

[15] K. Ouchi, T. Suzuki, and M. Doi, "LifeMinder: A wearable healthcare support system using user's context," in *Proc. Int. Conf. Distrib. Comput. Syst.*, 2002, pp. 791–792.

[16] Y.-J. Hong, I.-J. Kim, S. C. Ahn, and H.-G. Kim, "Activity recognition using wearable sensors for elder care," in *Proc. Int. Conf. Future Gener. Commun. Netw.*, 2008, pp. 302–305.

[17] P. Jiang *et al.*, "An intelligent information forwarder for healthcare big data systems with distributed wearable sensors," *IEEE Syst. J.*, vol. 10, no. 3, pp. 1147–1159, Sep. 2016.

[18] R. R. Fletcher, S. Tam, O. Omojola, R. Redemske, and J. Kwan, "Wearable sensor platform and mobile application for use in cognitive behavioral therapy for drug addiction and PTSD," in *Proc. IEEE Int. Conf. Eng. Med. Biol. Soc. (EMBC)*, 2011, p. 1802.

[19] J. Howell, A. Nag, M. McKnight, S. Narsipur, and O. Adelegan, "A low-power wearable substance monitoring device," in *Proc. Appl. Commercial Sensors*, 2016, pp. 1–9.

[20] J. B. Wang *et al.*, "Wearable sensor/device (fitbit one) and SMS text-messaging prompts to increase physical activity in overweight and obese adults: A randomized controlled trial," *Telemed. J. E-Health J. Amer. Telemed. Assoc.*, vol. 21, no. 10, pp. 782–792, 2015.

[21] J. Kim *et al.*, "Non-invasive alcohol monitoring using a wearable tattoo-based iontophoretic-biosensing system," 2016.

[22] R. Norris, D. Carroll, and R. Cochrane, "The effects of physical activity and exercise training on psychological stress and well-being in an adolescent population," *J. Psychosom. Res.*, vol. 36, no. 1, pp. 55–65, 1992.

[23] M. Lin *et al.*, "BeWell+: Multi-dimensional wellbeing monitoring with community-guided user feedback and energy optimization," in *Proc. ACM Conf. Wireless Health*, 2012, pp. 1–8.

[24] F. H. Wilhelm and W. T. Roth, "The somatic symptom paradox in DSM-IV anxiety disorders: Suggestions for a clinical focus in psychophysiology," *Biol. Psychol.*, vol. 57, nos. 1–3, p. 105, 2001.

[25] T. Roh, K. Bong, S. Hong, H. Cho, and H. J. Yoo, "Wearable mental-health monitoring platform with independent component analysis and nonlinear chaotic analysis," in *Proc. IEEE Eng. Med. Biol. Soc.*, 2012, pp. 4541–4544.

[26] M. Vidal, J. Turner, A. Bulling, and H. Gellersen, "Wearable eye tracking for mental health monitoring," *Comput. Commun.*, vol. 35, no. 11, pp. 1306–1311, 2012.

[27] A. Lanata, G. Valenza, M. Nardelli, C. Gentili, and E. P. Scilingo, "Complexity index from a personalized wearable monitoring system for assessing remission in mental health," *IEEE J. Biomed. Health Inform.*, vol. 19, no. 1, pp. 132–139, Jan. 2015.

[28] H. Lu *et al.*, "StressSense: Detecting stress in unconstrained acoustic environments using smartphones," in *Proc. ACM Ubicomp*, 2012, pp. 351–360.

[29] J. A. Naslund, K. A. Aschbrenner, and S. J. Bartels, "Wearable devices and smartphones for activity tracking among people with serious mental illness," *Mental Health Phys. Activity*, vol. 10, pp. 10–17, Mar. 2016.

[30] F. H. Wilhelm and P. Grossman, "Emotions beyond the laboratory: Theoretical fundaments, study design, and analytic strategies for advanced ambulatory assessment," *Biol. Psychol.*, vol. 84, no. 3, pp. 552–569, 2010.

[31] M. S. Mast *et al.*, "Social sensing for psychology: Automated interpersonal behavior assessment," *Current Directions Psychol. Sci.*, vol. 24, no. 2, pp. 154–160, 2015.

[32] P. Kakria, N. K. Tripathi, and P. Kitipawang, "A real-time health monitoring system for remote cardiac patients using smartphone and wearable sensors," *Int. J. Telemed. Appl.*, vol. 2015, Dec. 2015, Art. no. 373474, doi: 10.1155/2015/373474.

[33] A. Gaggioli and G. Riva, "From mobile mental health to mobile well-being: Opportunities and challenges," *Stud. Health Technol. Informat.*, vol. 184, pp. 141–147, 2013.

[34] F.-T. Sun *et al.*, "Activity-aware mental stress detection using physiological sensors," in *Proc. MobiCASE*, vol. 23, 2010, pp. 211–230.

[35] E. Ertin *et al.*, "AutoSense: Unobtrusively wearable sensor suite for inferring the onset, causality, and consequences of stress in the field," in *Proc. ACM Conf. Embedded Netw. Sensor Syst.*, 2011, pp. 274–287.

[36] V. W. S. Tseng *et al.*, "Assessing mental health issues on college campuses: Preliminary findings from a pilot study," in *Proc. ACM Int. Joint Conf. Pervasive Ubiquitous Comput.*, 2016, pp. 1200–1208.

[37] O. Lederman, A. Mohan, D. Calacci, and A. S. Pentland, "Rhythm: A unified measurement platform for human organizations," *IEEE MultiMedia*, vol. 25, no. 1, pp. 26–38, Jan./Mar. 2018.

[38] J. Gu *et al.*, "Wearable social sensing: Content-based processing methodology and implementation," *IEEE Sensors J.*, vol. 7, no. 1, pp. 7167–7176, Nov. 2017.

[39] D. Watson, L. A. Clark, and A. Tellegen, "Development and validation of brief measures of positive and negative affect: The PANAS scales, "*J. Pers. Soc. Psychol.*, vol. 54, no. 6, pp. 1063–1070, 1988.

[40] C. D. Spielberger, *STAI Manual for the State-Trait Anxiety Inventory: Self-Evaluation Questionnaire*. Palo Alto, CA, USA: Consult. Psychol. Press, 1970, pp. 1–24.

[41] R. R. Mccrae, "The NEO-PI/NEO-FFI manual supplement," 1989.

[42] M. Rosenberg, "Self esteem and the adolescent. (Economics and the social sciences: Society and the adolescent self-image)," *New England Quart.*, vol. 148, no. 2, pp. 177–196, 1965.

[43] M. A. Whisman, J. E. Perez, and W. Ramel, "Factor structure of the beck depression inventory-second edition (BDI-II) in a student sample," *J. Clin. Psychol.*, vol. 56, no. 4, pp. 545–551, 2000.

[44] S. Baron-Cohen *et al.*, "The autism-spectrum quotient (AQ): Evidence from asperger syndrome/high-functioning autism, males and females, scientists and mathematicians," *J. Autism Develop. Disord.*, vol. 31, no. 6, p. 603, 2001.
[45] A. Zanella, N. Bui, A. Castellani, L. Vangelista, and M. Zorzi, "Internet of Things for smart cities," *IEEE Internet Things J.*, vol. 1, no. 1, pp. 22–32, Feb. 2014.
[46] Y.-L. Hsu, S.-C. Yang, H.-C. Chang, and H.-C. Lai, "Human daily and sport activity recognition using a wearable inertial sensor network," *IEEE Access*, vol. 6, pp. 31715–31728, 2018, doi: 10.1109/ACCESS.2017.
[47] A. K. Das *et al.*, "Design of secure and lightweight authentication protocol for wearable devices," *IEEE J. Biomed. Health Inform.*, vol. 22, no. 4, pp. 1310–1322, Jul. 2018.
[48] A. K. Das, S. Zeadally, and M. Wazid, "Lightweight authentication protocols for wearable devices," *Comput. Elect. Eng.*, vol. 63, pp. 196–208, Oct. 2017.
[49] J. Srinivas, A. K. Das, N. Kumar, and J. Rodrigues, "Cloud centric authentication for wearable healthcare monitoring system," *IEEE Trans. Depend. Secure Comput.*, to be published, doi: 10.1109/TDSC.2018.2828306.

Sihao Yang received the B.Sc. degree from the School of Automation Engineering, Northeastern University, Qinhuangdao, China, in 2017. He is currently pursuing the M.Sc. degree in control engineering and science at the University of Electronic Science and Technology of China, Chengdu, China.

His current research interest includes wearable sensors.

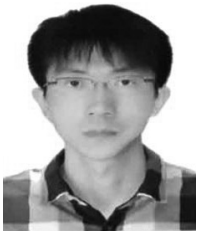

Bin Gao (M'12–SM'14) received the B.Sc. degree in communications and signal processing from Southwest Jiao Tong University, Chengdu, China, in 2005 and the M.Sc. degree (with Distinction) in communications and signal processing and the Ph.D. degree from Newcastle University, Newcastle upon Tyne, U.K., in 2011.

From 2011 to 2013, he was a Research Associate with Newcastle University, where he was involved with wearable acoustic sensor technology. He is currently a Professor with the School of Automation Engineering, University of Electronic Science and Technology of China, Chengdu. He has coordinated several research projects from the National Natural Science Foundation of China. His work has been actively published. His current research interests include sensor signal processing, machine learning, social signal processing, nondestructive testing and evaluation.

Dr. Gao is also a Reviewer for many international journals and long standing conferences.

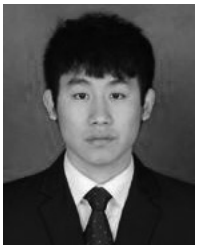

Long Jiang received the B.Sc. degree from the School of Information Engineering, Southwest University of Science and Technology, Mianyang, China, in 2012. He is currently pursuing the M.Sc. degree in control engineering and science at the University of Electronic Science and Technology of China, Chengdu, China.

His current research interests include intelligent hardware and wearable sensors.

Jikun Jin received the B.Sc. degree from the University of Electronic Science and Technology of China, Chengdu, China, in 2017, where he is currently pursuing the M.Sc. degree in speech scene recognition and machine translation.

Zhao Gao was born in Sichuan, China, in 1974.

She is an Associate Professor with the School of Foreign Languages, University of Electronic Science and Technology of China, Chengdu, China. From 2012 to 2014, she was an Academic Visitor with the MRC Cognition and Brain Sciences Unit, Cambridge, U.K., and the University of New Mexico, Albuquerque, NM, USA. Her current research interests include neuroendocrinological mechanism of metaphor bias in social and emotional contexts, foreign language classroom anxiety, and English for academic purpose reading pedagogy.

Xiaole Ma received the B.Sc. degree in applied psychology from Taiyuan Normal University, Taiyuan, China, in 2012. She is currently pursuing the Ph.D. degree in biomedical engineering at the University of Electronic Science and Technology of China, Chengdu, China.

Her current research interests include cognitive and affective neural science and data analysis.

Wai Lok Woo received the B.Eng. degree (First Class Hons.) in electrical and electronics engineering and the Ph.D. degree from Newcastle University, Newcastle upon Tyne, U.K.

He is currently a Senior Lecturer and the Director of Operations with the School of Electrical and Electronic Engineering, Newcastle University. He has authored or co-authored over 250 papers in various journals and international conference proceedings. He has an extensive portfolio of relevant research supported by a variety of funding agencies. His current research interests include the mathematical theory and algorithms for nonlinear signal and image processing, machine learning for signal processing, blind source separation, multidimensional signal processing, and signal/image deconvolution and restoration.

Mr. Woo was a recipient of the IEE Prize and a British scholarship to continue his research work. He is currently an Associate Editor of several international journals and has served as a Lead Editor for special issues of journals.